Yielding and Strain-Hardening of Reinforcement Materials

Ke Han, Vince Toplosky, Na Min, Yan Xin, Robert Walsh, and Jun Lu

***Abstract*—Part of the process for fabricating high field magnets using exceptionally strong reinforcement materials involves subjecting these materials to deformation at room temperature beyond the yield point. During the operation of the magnets, further plastic deformation may also occur at cryogenic temperatures. In most face-centered-cubic (fcc) materials, strain-hardening occurs after plastic deformation, further increasing strength. This paper reviews some of our recent work concerning the effect of microstructure on both yielding and strain-hardening in 316LN, a modified stainless steel, and in Haynes 242, a Ni–Mo–Cr alloy. Although both materials have fcc matrix, Haynes 242 yielded at higher stress with a lower strain hardening rate than 316LN at a low strain range. Because of high nitrogen content, 316LN showed pronounced yield point elongation. At cryogenic temperatures, both materials showed higher strain-hardening rates.**

***Index Terms*—High strength materials, reinforcement, failure mode, plastic deformation.**

I. Introduction

REINFORCEMENT materials have become more important as higher magnet fields have become possible [1]–[13]. The search for those materials has turned up various commercial alloys, previously invented for other purposes, which now need to be properly evaluated for application in high field magnets (HFMs). Two important parameters for assessing these alloys are the degrees of yielding and of strain-hardening. Reinforcement materials need both high yield strength and high strain-hardening rates in order to carry a heavy load in the coil and to avoid excessive plastic strain in the conductors. Certain high field magnets are usually operated at cryogenic temperatures, so the cryogenic properties of the reinforcement materials must also be assessed properly [2]–[4], [13]. Austenitic stainless steels have been widely used in the past as reinforcement materials [14]–[20]. Their database is relatively mature. In general, however, their yield strength is mediocre (e.g., below 1000 MPa at cryogenic temperatures). To achieve more desirable yield strength in materials for next generation HFMs, conventional austenitic stainless steels will have to be replaced [21]. Inventing or modifying these replacements will require a significant investment. Finding other reinforcement materials by repurposing existing materials is an attractive economic option. Many promising new alloys were originally developed for high-temperature applications, so they usually contain high-modulus elements, which tend to have high yield strength and high strain-hardening rate. This paper evaluates and compares the advantages and disadvantages of using austenitic stainless steel (a modified form of 316LN) as opposed to a high-temperature, nickel-based alloy (Haynes 242). Various nickel-based alloys have been considered before. Most nickel-based alloys were invented for high temperature applications. Recent work indicates that they can also be used at cryogenic temperatures for reinforcement materials for HFMs. Haynes 242 was selected for this study because of its high modulus, high strength, high fracture toughness, low crack growth-rate, and low thermal expansion coefficient.

Manuscript received December 26, 2018; accepted March 9, 2019. Date of publication March 27, 2019; date of current version May 1, 2019. The work was undertaken in the National High Magnetic Field Laboratory, which is supported by NSF DMR-1644779 and NSF DMR-1157490, the State of Florida, and DOE. *(Corresponding author: Ke Han.)*

K. Han, V. Toplosky, Y. Xin, R. Walsh, and J. Lu are with the National High Magnetic Field Laboratory, Tallahassee, FL 32309 USA (e-mail: han@magnet.fsu.edu; Toplosky@magnet.fsu.edu; Xin@magnet.fsu.edu; Walsh@magnet.fsu.edu; Junlu@magnet.fsu.edu).

N. Min is with Shanghai University, Shanghai 200444, China (e-mail: minnacyhome@126.com).

Color versions of one or more of the figures in this paper are available online at http://ieeexplore.ieee.org.

Digital Object Identifier 10.1109/TASC.2019.2907869

II. Experimental Methods

A. Materials

The typical chemistry of the modified stainless steel 316 LN is shown in Table I. One of the most important parameters is the content of the interstitial elements, i.e., carbon and nitrogen.

Previous work indicates that high carbon content can enhance the mechanical strength of the stainless steels but reduce the fracture toughness at cryogenic temperatures. In most of our cases, the carbon content is kept low.

The typical chemistry of Haynes 242 is also shown in Table I. Because of the high nickel content, the material remains as a face-centered cubic (fcc) phase at most fabrication temperatures. Most fcc structured materials remains ductile at high strength. In some alloys processed under certain conditions, however, intermetallic compounds may form [22], [23]. This may reduce the toughness of the alloys for cryogenic applications.

B. Tensile Testing

Longitudinally oriented samples (i.e., their axis is parallel to the sheet rolling direction) were used to perform most tensile tests on a 100 kN MTS test machine. A cryostat was installed on the machine to immerse both samples and test fixture in liquid helium or liquid nitrogen so that data at cryogenic temperatures can be collected.

TABLE I
ALLOY CONTENT IN WT.%

Alloy	C	N	Mn	Si	P	S	Cr	Ni	Mo	Nb+Ta	P + S	Fe
316LN modified	0.005	0.15	1.51	0.28	0.011	0.009	17.2	13.1	2.1	0.08	0.02	Bal
Haynes 242	0.03	2.5	0.8	0.8	---	---	8	65	25	---	---	2

The ASTM E1450 standard was followed for tensile testing in displacement-control mode with nominal strain rates between 1×10^{-4} and 7×10^{-4}. Samples with a reduced middle section were used so that the plastic deformation occurred within the gage lengths between 22 mm and 38 mm. An extensometer was clipped on samples to measure strain. The measurements provided both engineering stress (s) and engineering strain (e). Strain hardening rate was estimated by ds/de.

C. Microstructure Examinations

Transmission Electron Microscopy (TEM) samples were prepared by sectioning the alloy to discs of 3-mm in diameter. Electro-polishing was performed using both Fischione Model 110 and TenuPol-5 twin-jet electro-polishers. During the polish, samples were immersed in a solution of nitric acid in methanol. The polish current was 28–32 mA, and the temperature was about 240 K. TEM work was undertaken in a JEOL JEM-2011 and an ARM200 Electron Microscope. An energy dispersive X-ray (EDX) spectrometer was used to measure the elemental composition. Other details can be found in our previous paper [15].

III. RESULTS

Most of the following results apply to materials that were either heat treated or deformed. In most cases, reinforcement alloys must undergo both processes during the manufacture of coils.

A. Yielding at Low Strain

Stainless steel samples in the annealed condition showed both upper and low yield points. Heat treatment at about 700 °C, the commonly used temperature for Nb_3Sn superconductor reaction, enhanced both the high and low yield points for our samples (Fig. 1). This enhancement phenomenon is similar to what has been previously observed in carbon steels [24], [25].

Some of our stress-strain curves also revealed a certain degree of yield point elongation (YPE), which are known to produce Lüders bands in carbon steels [24], [25]. Such YPE may result in stretcher-strain. Studying the mechanism of YPE, therefore, is very important for both the science of plastic deformation of reinforcement materials and for the engineering applications of such materials for HFM.

Most researchers attribute YPE in low-carbon steels to the segregation of interstitial elements (e.g., carbon and/or nitrogen). If carbon and nitrogen content are reduced in steels (by, say, wet hydrogen treatment) to extremely low values, samples may show no yield point at all. Consequently, YPE, when it occurs, must be attributed to an interaction between interstitial atoms and whatever dislocations are present. The yield point is created by the unpinning of dislocations from surrounding interstitial atoms. In our stainless steels, a high nitrogen content may be the reason for the presence of YPE and of upper and lower yield points. At 700 °C, the solubility of nitrogen in steel is reduced. This leads more nitrogen atoms to segregate toward nearby dislocations, resulting in enhancement of both YPE and yield strength

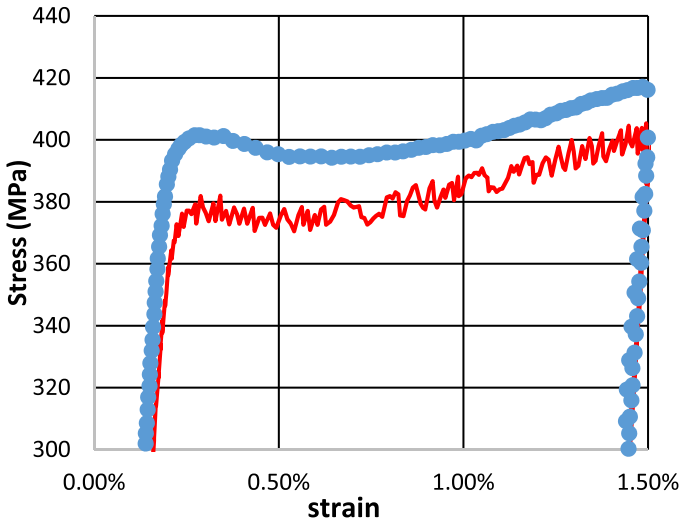

Fig. 1. Upper and lower yielding shown in stress-strain curves measured at room temperature for annealed, as-received 316 LN (thin solid line) and for aged 316 LN (thick solid line). Ageing was done at 700 °C for 100 hours. When both samples reach a strain of about 0.25%, softening occurs. The materials begin further hardening at strain values greater than 0.5%. The aged sample shows higher yield strength than the as-received sample. The ultimate tensile strength increases from 701 MPa before aging to 733 MPa after aging.

B. Deformation at High Strain

Stainless steels usually begin to plastically deform at a lower level of stress than nickel-based alloys (Fig. 2). Nickel-based alloys, on the other hand, do not even begin to plastically deform until a much higher level of stress is reached. Consequently, these alloys can reach much higher yield strength values than stainless steels.

C. Strain Hardening Comparisons

At low strain values (<2%), stainless steels exhibit high strain-hardening rates (Fig. 3). In this paper, the strain-hardening rate is the derivative of stress with respect to strain. At higher strain levels (>3%), the strain-hardening rate becomes relatively low, making it easier to deform the alloy for winding coils (for

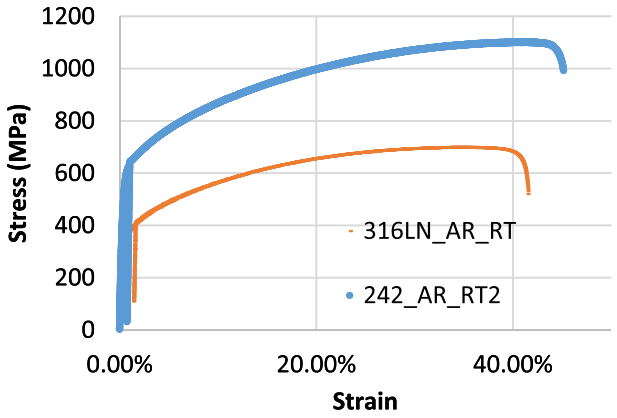

Fig. 2. Stress-strain curves of 316 LN stainless steel (thin orange curve) and Haynes 242 nickel-based alloy (thick blue curve) showing that the achievable yield strength of Haynes 242 is higher than that of 316LN. Both alloys were tested at room temperature in the annealed, as-received condition.

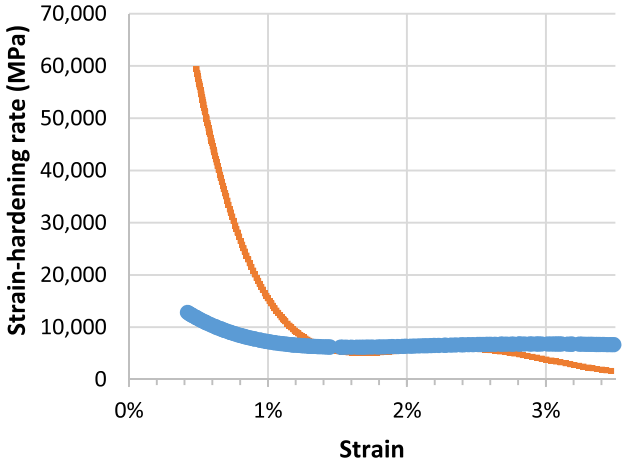

Fig. 4. Typical curves of the 4 K strain-hardening rate for 316 LN (thin solid orange line) and Haynes 242 (thick solid blue line). Both materials were aged at 700 °C for 100 hours.

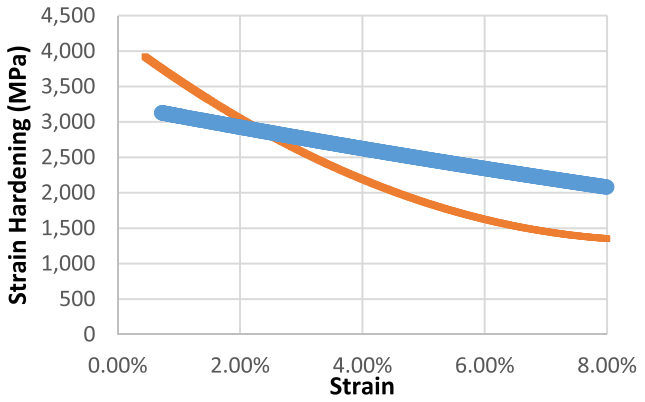

Fig. 3. Typical curves of room temperature strain-hardening rates for as-received (annealed) 316 LN (thin orange solid line) and Haynes 242 (thick blue solid line).

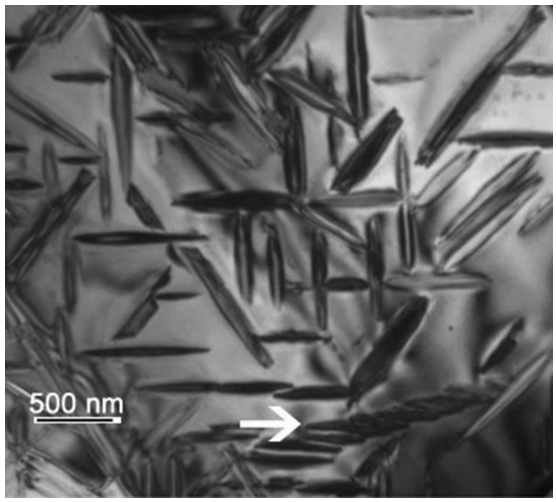

Fig. 5. TEM bright field image showing microstructure in aged Haynes 242. Contrasts in the image result from formation of NSHDs, which are oriented in four directions within a single grain. The arrowed region shows what appears to be a large NSHD oriented differently from the rest, but close examination reveals that it is actually composed of cluster of smaller close-packed NSHDs.

use as reinforcement) or for manufacturing conduits (for use in superconducting magnets).

Compared to stainless steels like 316 LN, certain nickel alloys like Haynes 242 have not only higher yield strength and higher Young's modulus but also higher strain hardening rates at large strain, (Fig. 3). The strain-hardening rate at a strain value of 3% was above 2500 MPa for the Haynes 242 studied in this work. The alloy has this higher strain-hardening rate because of its nickel content and because of its other high-modulus alloying elements (Mo and Cr).

D. 4 K Strain Hardening for Aged Alloys

In both 316 LN and Haynes 242, strain-hardening rates were higher at 4 K than at room temperature. This was because of the high dislocation accumulation rate produced by the suppression of dynamic recovery that occurs at low temperatures. At relatively low strain values, this suppression affected aged 316 LN more than aged Haynes 242. The 316 LN thus showed a higher strain-hardening rate at lower stress level (Fig. 4). When Haynes 242 was age-hardened, Ni_2Mo-type domains formed. These domains strengthened the alloy and increased yield strength. At this high stress level, activated dislocations needed only a moderate strain-hardening rate for their further movement. Therefore, at low strain, Haynes 242 had a lower strain-hardening rate than 316 LN.

Because the size of the domains in our aged samples was smaller than ~50 nm, the strengthening component was assumed to be nano-sized hardening domains (NSHDs) (Fig. 5). With the addition of Cr to form $Ni_2(Cr,Mo)$, the Ni_2Mo-type NSHDs became stable. The kinetics of $Ni_2(Cr,Mo)$ formation depended on heat treatment temperature; the lower the temperature, the slower the formation rate. For most superconductors, reaction temperature is between 600 °C and 700 °C. This temperature

range matches the full hardening temperature for Haynes 242, as well as for some other Ni-based alloys.

Previous researchers had identified only one orientation for Ni_2Mo-type NSHDs within the same grain [26]. Close examination of our samples, however, revealed four habit planes on which these NSHDs prefer to nucleate. These planes facilitate the growth of NSHDs in certain directions with respect to one another (Fig. 5). Because of these habit planes, property anisotropy is likely to develop in material that has undergone deformation, thus leading to variations in yield strength and strain-hardening rate.

IV. Discussion

During fabrication of reinforcement components for magnets (conduits for conductors and the like), materials are usually subjected to gradually increasing levels of deformation strain. Consequently, small and large strain values are equally important for the manufacture of high field magnets. This paper therefore discusses deformation of reinforcement materials to various strain values.

One of the advantages of using the stainless steel 316 LN in winding magnets is that, at room temperature, it has a relatively low strain-hardening rate at strain greater than 3%, as well as acceptable yield strength. This low strain-hardening rate and moderate yield point make it easier to fabricate the coil. Yield elongation, however, may induce surface defects in the early stage of deformation, making the material more susceptible to cyclic loading fatigue failure.

Although aged Haynes 242 has a low strain hardening rate at low strain, it has higher yield strength and a greater strain-hardening rate at large strain. Therefore, large forces are required to fabricate coils from aged Haynes 242. Lower force levels, however, can be employed when the method known as winding-and-hardening is used to make the coils from unaged Haynes 242. This means that the alloy before winding should be in an annealed or cold-deformed form so that both the yield strength and the strain-hardening rate remain moderate. In this manner, the winding force for manufacturing the magnet is reduced to an acceptable level.

Recently, other Ni-based alloys have been developed with even higher strength, higher hardness and higher modulus than Haynes 242. These alloys have various additional advantages over conventional alloys for the manufacture of high field superconducting magnets [27].

V. Summary

Modified stainless steels like 316 LN, because of their moderate strength, are deformed relatively easily at room temperatures and are widely used to fabricate magnet reinforcement components of various shapes. After aging, however, these steels, because of segregation of nitrogen, may show pronounced yield point elongation, which often leaves surface defects in the steel during the winding of magnet coils. Haynes 242, a Ni-based alloy, showed no yield point elongation and reached higher mechanical strength than 316LN. Nano-sized hardening domains (NSHDs), which occurred during aging, further enhanced the strength of Haynes 242. Other alloying elements also enhanced both strength and strain-hardening. These properties are desirable for reinforcing high field magnets but not ideal for winding magnet coils. Therefore, coils fabricated from Haynes 242 should be wound before age-hardening, i.e., before the formation of NSHDs.

Acknowledgment

The authors are grateful to Drs. D. Nguyen, J. Miller, M. Bird, and C. Mielke for their discussions of magnet design, and to Dr. M. Tyler for editing the manuscript.

References

[1] S. Askenazy, L. VanBockstal, F. Dupouy, and F. Herlach, "The performance of high-field magnets with optimized internal reinforcement," *Meas. Sci. Technol.*, vol. 7, no. 4, pp. 680–685, Jan. 1999, doi: 10.1088/0957-0233/7/4/026.

[2] K. Han *et al.*, "Material issues in the 100 T non-destructive magnet," *IEEE Trans. Appl. Supercond.*, vol. 10, no. 1, pp. 1277–1280, Mar. 2000, doi: 10.1109/77.828468.

[3] K. Han, J. R. Sims, C. A. Swanson, and H. J. Schneider-Muntau, "Reinforcement materials for high field magnets," *IEEE Trans. Appl. Supercond.*, vol. 14, no. 2, pp. 1141–1144, Jun. 2004, doi: 10.1109/TASC.2004.830449.

[4] K. Han *et al.*, "Selected ni alloy considerations for superconducting magnets," *IEEE Trans. Appl. Supercond.*, vol. 23, no. 3, Jun. 2013, Art no. 7800204, doi: 10.1109/TASC.2012.2235898.

[5] F. Herlach and M. von Ortenberg, "Pulsed magnets for strong and ultra-strong fields," *IEEE Trans. Magn.*, vol. 32, no. 4, pp. 2438–2443, Jul. 1996, doi: 10.1109/20.511366.

[6] F. Herlach, K. Rosseel, and J. Vanacken, "Frontiers of pulsed magnet design," *IEEE Trans. Appl. Supercond.*, vol. 14, no. 2, pp. 1229–1232, Jun. 2004, doi: 10.1109/TASC.2004.830537.

[7] A. S. Lagutin, K. Rosseel, F. Herlach, and Y. Bruynseraede, "Durable 70 T pulsed magnets," *Phys. B-Condens. Matter*, vol. 346, pp. 599–603, Apr. 2004, doi: 10.1016/J.PHYSB.2004.01.088.

[8] L. Li *et al.*, "High performance pulsed magnets with high strength conductors and high modulus internal reinforcement," *IEEE Trans. Appl. Supercond.*, vol. 10, no. 1, pp. 542–545, Mar. 2000, doi: 10.1109/77.828292.

[9] H. J. Schneider-Muntau, "Pulsed monocoil magnets for highest fields," *Current Appl. Phys.*, vol. 6, no. 1, pp. 54–58, Jan. 2006, doi: 10.1016/J.CAP.2005.01.049.

[10] H. J. Schneider-Muntau, K. Han, N. A. Bednar, C. A. Swenson, and R. Walsh, "Materials for 100 T monocoil magnets," *IEEE Trans. Appl. Supercond.*, vol. 14, no. 2, pp. 1153–1156, Jun. 2004, doi: 10.1109/TASC.2004.830461.

[11] C. A. Swenson *et al.*, "Performance of 75 T prototype pulsed magnet," *IEEE Trans. Appl. Supercond.*, vol. 16, no. 2, pp. 1650–1655, Jun. 2006, doi: 10.1109/TASC.2006.870551.

[12] C. A. Swenson, D. G. Rickel, and J. R. Sims, "80 T magnet operational performance and design implications," *IEEE Trans. Appl. Supercond.*, vol. 18, no. 2, pp. 604–607, Jun. 2008, doi: 10.1109/TASC.2008.922524.

[13] V. J. Toplosky and K. Han, "Mechanical properties of cold-rolled and Aged MP35N allloys for cryogenic magnet applications," in *Proc. Adv. Cryogenic Eng.*, vol. 58, vol. 1435, U. Balachandran, Ed., AIP Conference Proceedings, 2012, pp. 125–132.

[14] J. Bacon *et al.*, "First 100 T non-destructive magnet outer coil set," *IEEE Trans. Appl. Supercond.*, vol. 10, no. 1, pp. 514–517, Mar. 2000, doi: 10.1109/77.828285.

[15] K. Han, Y. Xin, R. Walsh, S. Downey, and P. N. Kalu, "The effects of grain boundary precipitates on cryogenic properties of aged 316-type stainless steels," *Mater. Sci. Eng. A*, vol. 516, no. 1-2, pp. 169–179, Aug. 2009. [Online]. Available: <Go to ISI>://000268424500026

[16] F. Lecouturier *et al.*, "Copper/stainless steel polyhelix magnets," *IEEE Trans. Appl. Supercond.*, vol. 22, no. 3, Jun. 2012, Art. no. 4300404.

[17] L. Li *et al.*, "Progress in the development of the wuhan high magnetic field center," *J. Low Temp. Phys.*, vol. 159, no. 1–2, pp. 374–380, Apr 2010.

[18] C. A. Swenson and W. D. Markiewicz, "Magnetic characterization of austenitic stainless steel for nuclear magnetic resonance coils," *IEEE Trans. Appl. Supercond.*, vol. 10, no. 1, pp. 736–739, Mar. 2000, doi: 10.1109/77.828337.

[19] M. R. Vaghar, L. Li, Y. Eyssa, H. J. Schneider-Muntau, and R. Kratz, "Roads to 100 T pulsed magnets," *IEEE Trans. Appl. Supercond.*, vol. 10, no. 1, pp. 507–509, Mar. 2000, doi: 10.1109/77.828283.

[20] H. Witte and H. Jones, "High-field magnet facilities and associated technology at Oxford," *Phys. B-Condens. Matter*, vol. 346, pp. 663–667, Apr. 2004, doi: 10.1016/J.PHYSB.2004.01.079.

[21] K. Han, Y. Xin, and R. P. Walsh, "An intermetallic precipitate strengthened alloy for cryogenic applications," in *Proc. Adv. Intermetallic-Based Alloys Extreme Environ. Energy Appl.*, M. Palm, B. P. Bewlay, Y. H. He, M. Takeyama, and J. M. K. Wiezorek. Eds., Materials Research Society Symposium Proceedings, vol. 1128, pp. 317–322, 2009.

[22] P. Mao, K. Han, and Y. Xin, "Thermodynamic assessment of the Mo–Re binary system," *J. Alloys Compounds*, vol. 464, no. 1–2, pp. 190–196, 2008.

[23] P. L. Mao, Y. Xin, K. Han, and W. G. Jiang, "Effects of heat treatment and Re-content on the TCP-phase in two Ni–Mo–Cr–Re superalloys," (in English), *(Acta Metall. Sin.-Engl. Lett.)*, vol. 22, no. 5, pp. 365–372, Oct. 2009, doi: 10.1016/s1006-7191(08)60110-6.

[24] B. Mintz, H. Ke, and G. D. W. Smith, "Grain-size strengthening in steel and its relationship to grain-boundary segregation of carbon," *Mater. Sci. Technol.*, vol. 8, no. 6, pp. 537–540, Jun. 1992, doi: 10.1179/MST.1992.8.6.537.

[25] Z. Y. Shen, B. L. Wang, G. F. Liang, Y. H. Zhang, K. Han, and C. J. Song, "Grain boundary pop-in, yield point phenomenon and carbon segregation in aged low carbon steel," *ISIJ Int.*, vol. 58, no. 2, pp. 373–375, 2018.

[26] Haynes International. Accessed: Feb. 2, 2019. [Online]. Available: https://www.haynesintl.com/alloys/alloy-portfolio/High-temperature-Alloys/HAYNES-242-Alloy/principal-features.aspx

[27] P. L. Mao, Y. Xin, and K. Han, "Anomalous aging behavior of a Ni–Mo–Cr–Re alloy," (in English), in *Proc. Mater. Sci. Eng. A-Struct. Mater. Properties Microstructure Proc.*, vol. 556, pp. 734–740, Oct. 2012, doi: 10.1016/J.MSEA.2012.07.057.